2003

Steps Toward the Creation of a Carbon Nanotube Single Electron Transistor

R. Matthew Ferguson
Pomona College

Steps Toward the Creation of a Carbon Nanotube Single Electron Transistor.

R. Matthew Ferguson

Submitted in partial fulfillment of the requirements for the degree of Bachelor of Arts in Physics, Pomona College
Wednesday, 7 May, 2003

Advised by: Dr. David Tanenbaum

Table of Contents

Abstract

This report details work toward the fabrication of a single-electron transistor created from a single-walled carbon nanotube (SWNT). Specifically discussed is a method for growing carbon nanotubes (CNTs) via carbon vapor deposition (CVD). The growth is catalyzed by a solution of 0.02g $Fe(NO_3)_3 \cdot 9H_2O$, 0.005g $MoO_2(acac)_2$, and 0.015g of alumina particles in 15mL methanol. SWNT diameter ranges from 0.6 to 3.0 nm. Also discussed is a method to control nanotube growth location by patterning samples with small islands of catalyst. A novel "maskless" photolithographic process is used to focus light from a lightweight commercial digital projector through a microscope. Catalyst islands created by this method are approximately 400 μm^2 in area.

Chapter 1: Introduction

Carbon nanotubes (CNTs) were discovered in 1991 by S Iijima of the NEC Lab of Japan, who stumbled upon the tiny carbon ropes while looking for Fullerene molecules in the ashes made by arc-discharge. Since their discovery nanotubes have become the darling of many solid-state and nanoscience labs because of their tiny size and remarkable physical properties: nanotubes are conductive, and can behave as metals or semiconductors. Single-walled nanotubes (SWNTs) have diameters between 0.75 and 5nm, and lengths up to many μm. Nanotubes are also exceptionally strong, with measurements of some tubes indicating a high Young's modulus $Y = 1.25 - 0.35/+0.45\,\text{TPa}$.[1]

Myriad applications for CNTs have been proposed, both clever and absurd: nanotubes could be used to store hydrogen at near liquid density in hydrogen fuel cells, or as field-emitters in the next generation of electronic displays. In batteries they could prolong the life of anodes and cathodes. Electrical circuits could be made with molecular-sized nanotube transistors and logic gates, why not even an entire nanotube random access memory? Ropes and bundles of tubes could be used as ultra-strong structural components in buildings or aircraft. A more fanciful application involves using nanotubes—the first material to be strong enough—in the construction of a continuous elevator into earth's orbit, ushering in the obsolescence of conventional rocketry.

CNTs provide interesting physics problems even while they prod the imagination. SWNTs are essentially 1D wires that exhibit extreme sensitivity to structural changes. Reversible structural deformations such as bending or stretching can temporarily change the conductance of a nanotube by orders of magnitude. One of the physics problems to

which the enumerated properties of CNTs are suitable is Coulomb blockade, and this is the project which we set out to accomplish, and in whose scope the completion of my work is but a part.

It is possible to induce local structural deformations into a nanotube that create a tunnel barrier. This can be done in several ways with an atomic force microscope. If a tube wall is bent violently enough that it folds or buckles, conventional current flow is arrested, and electrons must tunnel across the barrier. Dekker et al. have observed that making two such kinks in close proximity on the same nanotube creates a oulomb island. [2] By gating the substrate beneath the nanotube they create a single-electron transistor at room temperature. We wish to show that it is possible to create a similar device, where tunnel barriers are made by pulsing a voltage near a nanotube to partially destroy the tube wall.

1.1 Project Outline

Much work was required before this project could be completed in our lab, much more than I could complete. Since I could only focus on a few aspects of the project, an outline of the remaining work follows.

The first step was the development of a reliable method for growing CNTs. Preferably this method would allow growth to be directed so that nanotubes could be grown in a similar configuration on subsequent samples, allowing the electrode design to remain fixed. Without a fixed electrode pattern a great deal of work must be spent finding nanotubes and re-designing electrodes for each sample, wasting many hours when large numbers of samples must be produced. A relatively straightforward way to direct

nanotube growth is by lithographically patterning the deposition of catalyst used in CVD growth.

After consistent samples can be produced, macroscopic electrodes must be brought into contact with CNTs on the sample surface. In a CVD growth scheme, the easiest way to create electrodes is to deposit metal films on top of grown nanotubes. Once a tube has been properly connected to two electrodes its electrical properties can be measured.

To create a Coulomb Blockade device, a Coulomb island must be created in the nanotube. Applying a voltage pulse near the walls of a SWNT causes electrons in the molecules of the tube wall to accelerate rapidly, breaking bonds and damaging the tube structure. Such localized pulses can be generated by applying voltage to a conductive AFM tip. If the pulse is too strong the tube walls will be fully destroyed, but a carefully applied pulse will break only some bonds, leaving others intact. Because electron flow is regulated by quantum effects produced by the tube geometry, such defects can stop conventional electron flow and create a tunnel barrier. If a second defect is introduced to the same nanotube, the region between the tunnel barriers becomes a Coulomb Island.

Construction of the Coulomb blockade device is completed by applying a gate voltage to the substrate beneath the island (it is also possible to generate a gate voltage with an AFM tip brought near the island.) and a bias voltage to the nanotube ends. Measurements of the differential conductance dI/dV show a periodic dependence on gate voltage, that does not exist before the island is created.[2] This dependence is a feature of Coulomb blockade.

[1] Yakobson, B. I., and Avouris, Ph. **Mechanical Properties of Carbon Nanotubes.** M.S. Dresselhaus, G. Dresselhaus, Ph Avouris (Eds.): *Carbon Nanotubes*, Topics Appl. Physics. 80, 287-329 (2001)
[2] Postma, H. W. Ch., Teepen, T., Yao, Z., Grifoni, M., and Dekker, C. **Carbon Nanotube Single-Elecron Transistors at Room Temperature.** *Science.* Vol. 293, 76-79 (2001)

Chapter 2: Theory

2.1 Structure and Electronic Properties of SWNTs

SWNTs have the same geometry as a rolled strip of graphene. Figure 1 maps the basic geometry of tube roll-up. The tube can be rolled up in several configurations, described by the roll-up vector $c_h = na_1 + ma_2$, where $\mathbf{a_1}$ and $\mathbf{a_2}$ are graphene lattice vectors and *(n,m)* are integers.

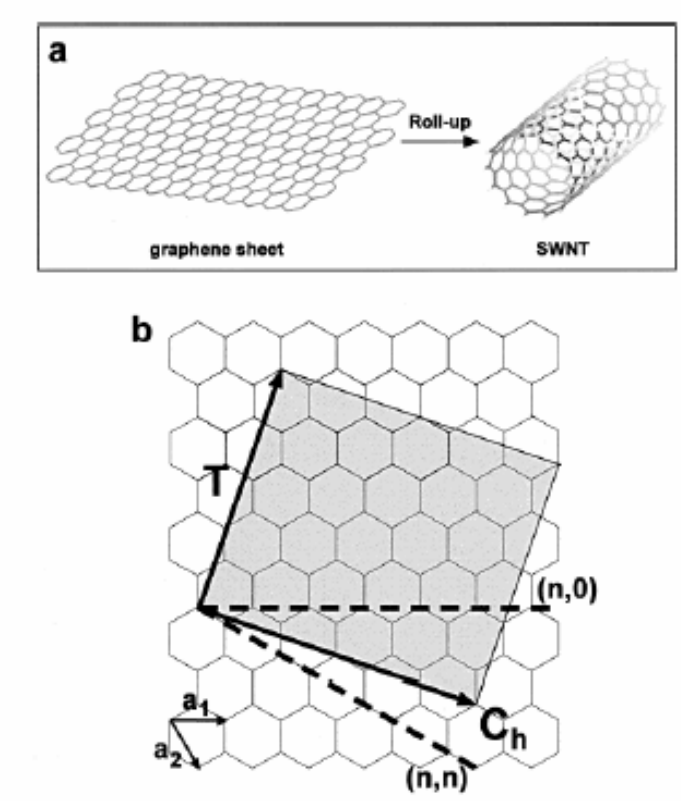

Figure 1.[1]

A tube's geometry is specified by the roll up vector $c_h = na_1 + ma_2$, *where* a_1 *and* a_2 *are the graphene lattice vectors connecting crystallographically equivalent sites on the 2-D sheet, and (n, m) are integers.* $\mathbf{C_h}$ *is set up as (n, m) = (4,2) in this figure and* T *is directed along the nanotubes axis and orthogonal to* c_h.

The grey area of figure 1b is the repeat unit, or unit cell of an (*n,m*) tube. The dotted lines represent the limiting cases referred to as zigzag (*n,0*), and armchair (*n,n*).

The electronic properties of a SWNT are very sensitive to differences in the available geometries. This sensitivity is due to the band structure of graphene, and the quantization of electron momentum around the circumference of a tube. The conducting and valence bands of graphene overlap only at six degenerate points—called **K** (k_F) points—located at the corners of the first Brillouin zone. A representation of the π and π^* bands and their overlap at the **K** points is given in figure 3a and 4a. As a piece of 2D graphene is rolled into a 1D tube, periodic boundary conditions are imposed along the tube's circumference. These can be expressed in terms of the vector $\mathbf{c_h}$ as:

$$c_h \bullet k = 2\pi q \qquad (1)$$

where q is an integer. The parallel white lines of figures 2b, 3b, and 3c, are the allowed subbands that satisfy eq. 1 in reciprocal space along the tube axis, and the allowed states for an (n,m) tube lie along these lines.[1] A detailed discussion of the band structure of SWNTs can be found in [1].

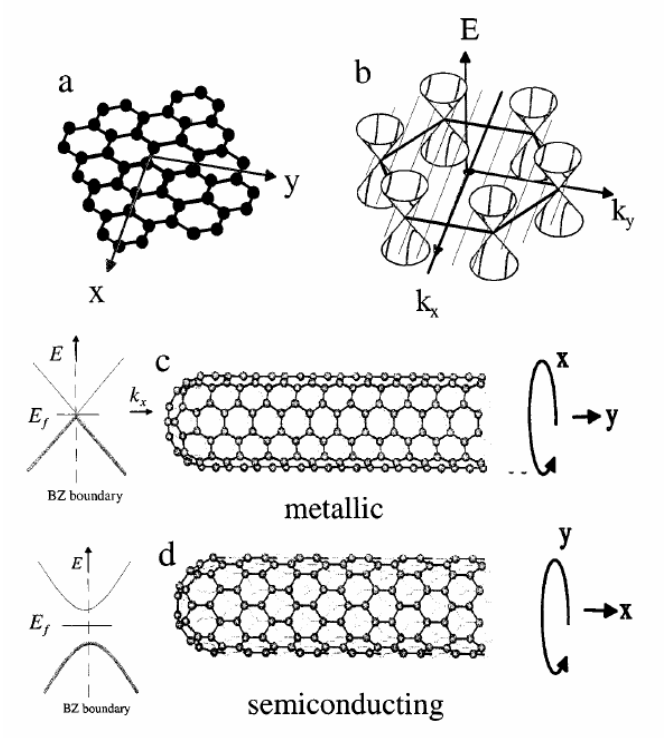

Figure 2.[2]

Figure 2b shows that the conducting states of graphene as a function of wavevector k, exist only in cones along certain directions. Figure 2c,d depict the structure and band gap of metallic and semiconducting tubes.

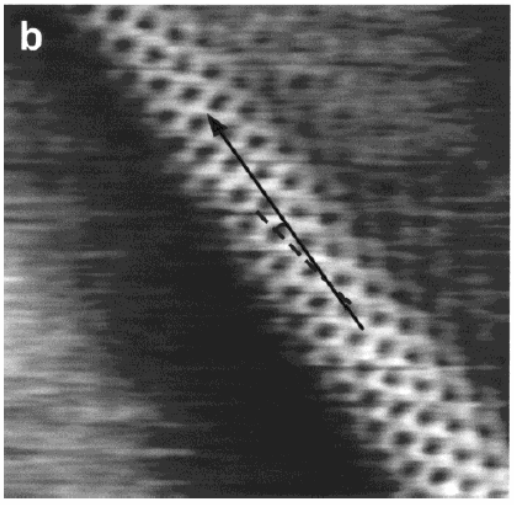

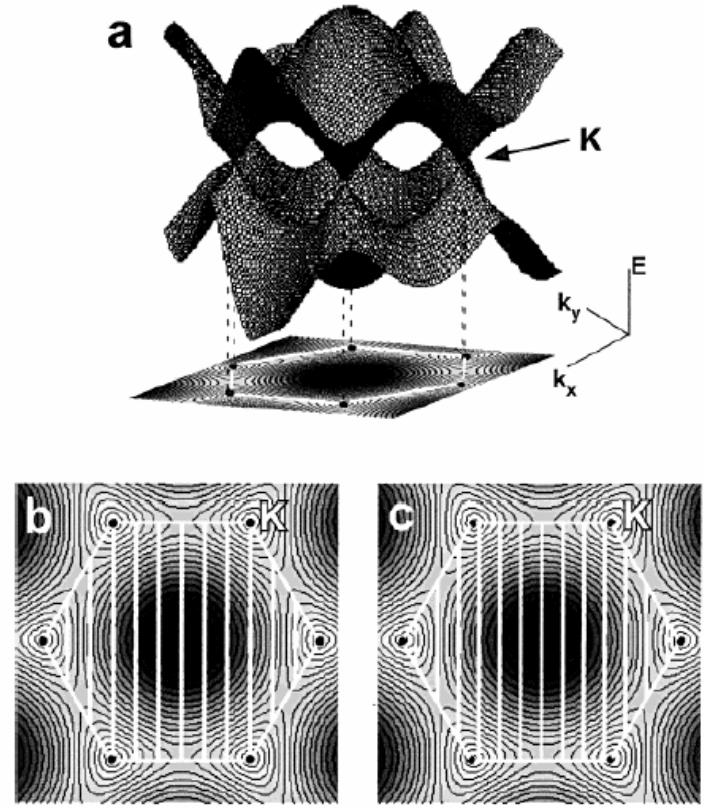

Figure 3.[1]

*A three dimensional depiction of the π/π^* bands in graphene. The dips in this figure correspond to the cones of Fig. 2b. 3b shows the 1D subbands of a (9,0) metallic nanotube and 3c shows a (10,0) semiconducting tube. The white hexagon defines the first Brillouin zone of graphene. The black dots are **K** points. Note that the allowed subbands of the metallic tube include **K** points, and those of the semiconducting tube do not.*

Figure 4.[1]

STM image of SWNT. The arrow shows the tube axis, and the dotted line the zigzag direction.

If the allowed subbands include a **K** point, as in figure 3b, then the nanotube will be metallic. Thus equation one becomes the condition for metallic tubes

$$c_h \bullet k_F = 2\pi q \qquad (2)$$

If no subband passes through a **K** point, as in figure 3c, then the nanotube is semiconducting. Tubes with indices (*n,n*) and (*n,0*) are metallic. (*n,m*) tubes with $n - m = 3j$, where *j* is a nonzero integer, are tiny-gap semiconductors, and all others are large-gap semiconductors.[3] Tubes with $n - m = 3j$ would be metals if we considered only the band scheme, but small curvature effects due to roll-up introduce a tiny energy gap to the band structure. As tube radius R increases, the band gaps of both the large-gap and tiny-gap semiconducting tubes decrease with $1/R$ and $1/R^2$, respectively. This dependence means that all but the narrowest tiny-gap ($n - m = 3j$) tubes will be difficult to distinguish from metallic tubes at room temperature.[3]

2.2 Growth of SWNTs

Carbon Nanotubes can be grown by three methods. During arc-discharge and laser ablation, CNTs are formed during the evaporation of carbon atoms from solid carbon sources at temperatures between three and four thousand degrees centigrade. We are mostly interested here in the third method, carbon vapor deposition (CVD). During CVD growth, CNTs are formed when a hydrocarbon gas flows over catalyst material that has been heated to 700-1000º.

Growth can be made to occur at different temperatures with a variety of hydrocarbon sources and catalyst materials. Following Dai, et al.[4], we have chosen to use Methane as our carbon source, and a mixture of Fe and Mo supported on alumina as our

catalyst. The motivation for these material selections can be explained by a general discussion of tube growth.[5]

During the CVD process, the hydrocarbon source is disassociated by the presence of a small particle of metal catalyst. Dissolved carbon atoms then diffuse into the metal, forming a metal-carbon solution. When the particle becomes super-saturated, the dissolved carbon can precipitate in the energetically favorable tube form. For this method to work properly, the catalyst must be able to form a carbon-metal solution at high temperature; transition metals such as Fe, Co, Ni, and Mo all work well as catalysts.

The number of tubes that can be grown is clearly related to the number of catalytic sites available. For this reason the metal catalyst can be mixed with a support material—such as Alumina—that increases the surface area to which catalyst can adhere. A good support material strongly interacts with the metal catalyst, binding catalyst particles to most of its surface area. Strong metal-catalyst interaction increases the number of nucleation sites and discourages the formation of large aggregate metal particles. Smaller metal particles are doubly desirable because the diameter of a SWNT usually parallels that of the catalyst particle. Despite these benefits to adding a support material, significant nanotube growth can also be realized on un-supported catalyst.[6]

Temperatures during growth are high enough that the reaction of catalyst metal with the substrate must be considered, specifically the reaction between iron and the silicon substrate to form FeSi, a silicide. In a study of CVD growth catalyzed by a layer of iron deposited directly onto silicon surface, the formation of silicide has been shown to inhibit the growth of nanotubes due to the reduced catalytic efficiency of iron silicide.[7]

The same study shows that this effect can be countered by reducing the percentage of iron catalyst that can react with the silicon surface. Such a reduction is accomplished effectively by depositing a layer of TiN on the silicon surface before iron deposition. Only a small amount of Si can diffuse through the dense TiN film to react with the Fe catalyst. It is also noted that increasing the thickness of the Fe layer leads to an increase in CNT production. Rather than reducing the amount of Si that can react with the catalyst, enough catalyst is deposited to make the Si interaction negligible. Too thick a Fe layer is also detrimental to CNT growth.[8]

I have noted that nanotubes grow in our furnace only on silicon samples with an oxide layer whose thickness is at least several microns. This observation is probably further evidence of silicide formation. The density of Si in SiO_2 is less than that of crystalline Si, reducing the number of Si atoms that can react with the Fe catalyst. The oxide layer acts as a buffer protecting some of the catalyst from silicide formation.

At growth temperatures hydrocarbon gasses tend to self-dissociate by pyrolysis. This process can compete with the catalyzed dissociation, and reduce the number of carbon atoms available for tube growth. Hydrocarbon pyrolysis is further problematic because it can lead to the formation of unwanted amorphous carbon, which can coat nanotubes and generally make a mess. Methane is the most stable hydrocarbon at high temperature, and therefore it lends itself well as a source gas.

Though it is the most stable hydrocarbon methane does have some tendency to disassociate, and in more recent work Dai, et al. have introduced a small amount of H_2 during growth to reduce methane pyrolysis.[9] H_2 is a product of CH_4 pyrolysis, so its presence during reaction slows down the decomposition of CH_4 by hydrogenating

reactive carbon molecules. As always, to be effective this process requires balance; too much H_2 presence will inhibit dissociation at the catalyst particles leading to reduction in tube formation.

2.3 Growth Mechanisms

Under most growth conditions both SWNTs and multi-walled nanotubes (MWNTs) are produced. In this study I focus on SWNTs, and I will also focus the discussion of growth mechanisms to the single shelled species. SWNTs can only be grown in the presence of a catalyst material,[10] whereas their multi-walled counterparts can be grown from a pure carbon source. This experimentally-derived fact suggests that the different types of tubes have different growth mechanisms.

While multi-walled nanotubes (MWNTs) seem to grow by the addition of carbon dimers to a stable, open tube end, open ended growth is unlikely for SWNTs. The stability of an open tube end is dependent on tube diameter. Above a critical value of about 3 nm open ends are stable, and growth can continue by the addition of carbon molecules to form new hexagons.[10] Pentagonal structures form readily on an open tube with diameter below the critical value, and these pentagons curve inward and rapidly close the tube. Carbon deposition on a closed tube end is disorderly, making it impossible for an ordered tube to grow from a closed end. SWNTs generally have diameters less than or equal to the critical value, so the open-ended mechanism is unlikely for SWNT growth.

From the knowledge that open ended tube growth is not possible for SWNTs, and SWNTs only grow in the presence of catalyst material, we can infer that catalyst particles

must play a direct role in the growth mechanism of SWNTs. The precise nature of this role is unclear, but there are two basic modes of growth which seem likely. In both models new carbon atoms are added to the tube structure through interaction with the metal catalyst, and the catalyst holds the tube open throughout growth by attaching to the dangling bonds at one tube end. The two basic models differ in the location of the catalyst.

In root, or base growth, it is proposed that the catalyst particle does not move significantly during growth; as carbon is added at the tube base the end moves away from the catalyst, much like a Fourth-of-July "snake." Within this model tube nucleation must be explained differently depending on the size of the involved catalyst particle. It was mentioned previously that SWNT diameters frequently match the diameter of the metal catalyst from which they grow, for catalyst particles of diameter between .5 and 3 nm. Fullerene molecules may form on the catalyst surface and be prevented from closing when catalyst atoms decorate their dangling bonds. As additional carbon atoms collide with the catalyst they are incorporated between metal and carbon shell, pushing the fullerene end-cap off the particle surface and forming a tube.[10] A depiction of such growth is found in figure 5. This model seems to match that proposed by Hongjie Dai[5] for Fe catalyst compounds, and mentioned in the previous section.

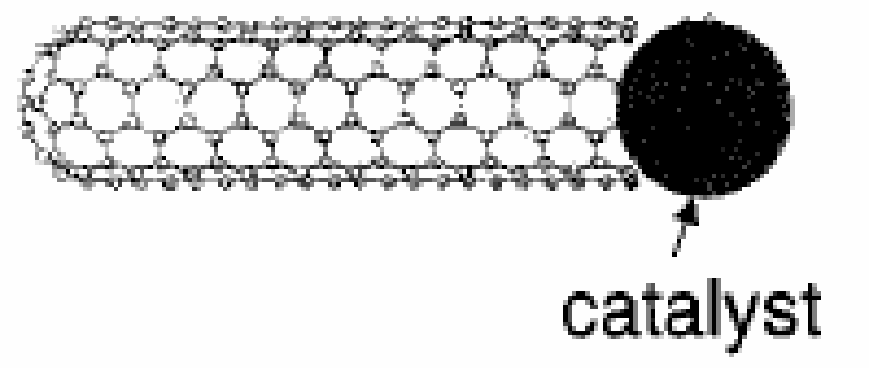

Figure 5.[2]
A depiction of the root growth model for catalyst particles of diameter approximately equal to nanotube diameter.

If the catalyst particle is larger than 3 nm, a fullerene dome cannot precipitate nanotube growth, and the diameter cannot be set by the particle size; SWNT growth must occur by a different mechanism. SWNTs have been observed to grow from particles much larger than 3 nm under arc discharge[10] (Similar growth may not be possible under CVD conditions, but this alternate root growth model is interesting to consider). Molecular-dynamics simulations[10] of the structure of SWNTs grown by this process show a bubble-like carbon shell protruding from the flat particle surface, with large positive curvature near the base. In this highly-curved region are found mostly heptagons that are energetically stable when highly curved. These heptagons interact with neighboring rings, especially pentagons, to produce hexagons at the tube base—resulting in defect free nanotubes growth.

The alternative to root growth involves a translating growth region that carries catalyst particles with it as new carbon is added to the nanotubes. Many plausible mechanisms have been proposed,[10] but I will limit discussion here to a closed-end catalytic growth mechanism because it contrasts nicely with the small-particle root growth model.

Though, as mentioned above, it is not possible for a SWNT to grow from a closed fullerene-like tube end, such growth becomes possible if a small Fe or Co molecule is incorporated into the apex of the closing tube. Unlike a closed tube of pure carbon, which is inert, bonds are continually broken and reformed at the metal-carbon junction. At such a junction new carbon could be absorbed from the vapor phase and introduced into the tube structure.[10]

Experimental observations do not frequently encounter nanotubes with metal particles embedded in their ends as this model would suggest. This chemical activity of the metal-carbon junction may also offer an explanation for these findings. Because these bonds are frequently broken it is possible that the particle is ejected completely, terminating tube growth. It is also possible that metal particles are in fact very small and so difficult to detect experimentally, in which case field emission and magnetic properties should be affected.[10]

Though several proposed models for understanding the role of catalyst materials in SWNT growth have been discussed, the actual role of catalyst during growth is not well-understood. Most studies of nanotubes to date have involved scouring for tubes in the debris left behind by the growth process. Experiments that monitor the actual growth process are now being performed, and should eventually improve our understanding of growth mechanisms.

2.4 Conductance: Defects, Junctions, Contacts

The conductance of a nanotube can be described using the Landauer-Buttiker Formula for systems of parallel 1D channels: $G = (Ne^2 / h)T$, where T is a transmission coefficient.

SWNTs with perfect contacts ($T=1$) have been shown to possess a fundamental contact resistance of about 6.5kΩ.[3] Imperfect contacts will give rise to an additional resistance R_c, and the nanotube has a resistance due to scattering of $R_t = (h/4e^2)(l/L)$, where l is the mean free path, and L is the tube length. The total tube resistance is the sum $R=G+R_c+R_t$.

Given the high sensitivity of nanotube electronics to geometry, it is not surprising that physical deformations in a tube wall can lead to changes in conductance. A study by Tombler et al. has shown that physical deformations—created simply by squashing a suspended nanotube with an AFM tip—can lead to a reduction in conductance of two orders of magnitude.[11] Dekker et al. have taken mechanical deformation one step further. By introducing a kink, or buckle, in the nanotube structure (again using an AFM tip) they create a nanometer-sized tunnel barrier.[12] They add a second barrier in the same tube to create a 25 nm Coulomb island, and measure Coulomb blockade, or single-electron tunneling. Adding a back gate voltage at the substrate below the nanotube allows them to modulate the conductance, turning their device into a single-electron transistor.

Other interesting devices can be created by joining nanotubes of different chirality to form metal-metal, metal-semiconductor, or semiconductor-semiconductor junctions. Such connections can be made in two different ways. In the first method, it is possible for the chirality of a nanotube to change at some point along its length if a defect is introduced in its structure. It has been shown that pentagon-heptagon pairs placed in the tube's network can lead to fundamental changes in electronic structure.[3]

Though the idea of joined nanotubes is interesting, it is difficult to synthesize such systems with consistency. The second method is more easily reproduced, and involves

crossing two or more nanotubes of different chirality. In free space crossed tube junctions are not pressed together with sufficient force to interact strongly; they remain at a van der Waals distance at their closest point of contact.[3] If the same intersection is brought to the surface of a substrate such as Si, the strong attraction between nanotube and substrate will press the two tubes together at their junction with a force of about 5nN, enough to deform the tube wall and increase the junction conductance.[3] In a calculation by McEuen et al. the effects of substrate interaction reduce the closest atomic separation of two (*5,5*) metallic nanotubes from the van der Waals distance of 0.34nm to 0.25nm, producing an junction conductance of about 5% of a quantum unit of conductance $G_0=2e^2/h$.[3,13] Figure 6 shows the crossed junction device fabricated by McEuen et al.

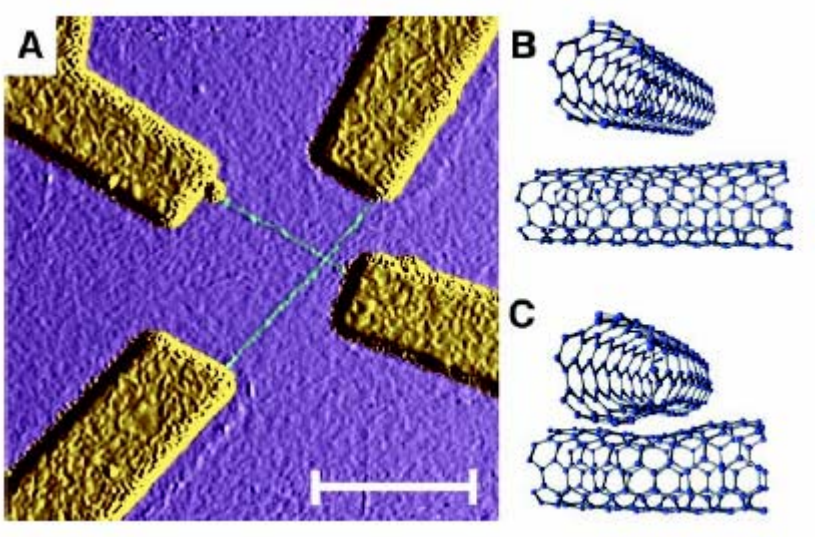

Figure 6.[13]

A shows two crossed nanotubes with gold contacts (scale bar ~150 nm). B,C show the structures used to calculate the conductance at the junction of two (5,5) metallic SWNTs. The change in structure caused by crossing tubes on a substrate can be seen in C.

Semiconductor-semiconductor junctions with conductance as high as 0.011 and 0.06 e^2/h were observed in the same study. The metal-semiconductor case is particularly

interesting. McEuen et al. predicted that a metal nanotube joined to a semiconducting tube will deplete the doping of the semiconducting tube at the junction, leading to Schottky Diode behavior. They observed a Schottky barrier of 200-300 meVin a metal-semiconductor junction, close to the expected value of 250 meV for 1.4 nm diameter nanotubes.[12] Other diode-like structures can be created from nanotube junctions, including both p and n-type CNT field-effect transistors.[14]

Though both p and n-type semiconducting nanotubes have been observed, most semiconducting nanotubes observed are unipolar p-type. This may in fact be due to effects at the electrode contact. Common methods for joining carbon nanotubes and electrodes involve depositing nanotubes onto a gold pattern, or depositing gold onto nanotubes. The contact of such junctions is typically poor, with high contact resistance (on the order of 1MΩ)—though recently this number has been dropped significantly, and is now as low as 10kΩ.[15] In addition to high contact resistance traditional contacts may have a particularly high barrier for n-type conduction. Thus the tendency for SWNTs to appear as p-type is a characteristic of the contact barrier, and not of conduction along the length of the tube. To corroborate this idea, recent study of TiC end-bonded contacts shows very low resistance to both p and n-type conduction as well as ambipolarity. [16]

---

[1] Odom, T. W., Huang, J-L., Kim, P., and Lieber, C. M. **Structure and Electronic Properties of Carbon Nanotubes.** *Journal of Physical Chemistry B* 104, 2794-2809 (2000)
[2] McEuen, P. L., Fuhrer, M., and Park, H. **Single-Walled Carbon Nanotube Electronics.** *IEEE Transactions on Nanotechnology,* 1, no. 1, 78-85 (2002)
[3] Louie, S. G. **Electronic Properties, Junctions, and Defects of Carbon Nanotubes.** M.S. Dresselhaus, G. Dresselhaus, Ph Avouris (Eds.): *Carbon Nanotubes*, Topics Appl. Physics. 80, 113-145 (2001)
[4] Kong, J., Soh, H. T., Cassell, A. M., Quate, C. F., and Dai, H. **Synthesis of Individual Single-Walled Carbon Nanotubes on Patterned Silicon Wafers.** *Nature* **395**, 878 - 881 (1998)
[5] Dai, H. **Nanotube Growth and Characterization.** M.S. Dresselhaus, G. Dresselhaus, Ph Avouris (Eds.): *Carbon Nanotubes*, Topics Appl. Physics. 80, 29-53 (2001)

[6] Hafner, J. H., Cheung, C.-L., Oosterkamp, T. H., and Lieber, C. M. **High-Yield Assembly of Individual Single-Walled Carbon Nanotube Tips for Scanning Probe Microscopies**. *The Journal of Physical Chemistry B* 105, 4, 743 (2001)

[7] de los Arcos, T., Vonau, F., Garnier, M. G., Thommen, V., Boyen, H.-G., and Oelhafen, P. **Influence of Iron-Silicon Interaction on the Growth of Carbon Nanotubes Produced by Chemical Vapor Deposition.** *Applied Physics Letters* vol. 80, no. 13, 2383-2385

[8] Sohn, J. I., Choi, C-J., Lee, S., and Seong, T-Y. **Growth Behavior of Carbon Nanotubes on Fe-Deposited (001) Si Substrates.** *Applied Physics Letters* vol.78, no. 20, 3130-3132

[9] Franklin, N. R., Li, Y., Chen, R. J., Javey, A., and Dai, H. **Patterned Growth of Single-Walled Carbon Nanotubes on Full 4-Inch Wafers.** *Applied Physics Letters* vol. 79, no. 27, 4571-4573

[10] Charlier, J-C, Iijima, Sumio. **Growth Mechanisms of Carbon Nanotubes**. M.S. Dresselhaus, G. Dresselhaus, Ph Avouris (Eds.): *Carbon Nanotubes*, Topics Appl. Physics. 80, 55-80 (2001)

[11] Tombler, T. W., Zhou, C., Alexseyev, L., Kong, J., Dai, H., Liu, L., Jayanthi, C. S., Tang, M., and Wu, S-Y. **Reversible Electromechanical Characteristics of Carbon Nanotubes Under Local-Probe Manipulation.** *Nature* **405**, 769-772 (2000)

[12] Postma, H. W. Ch., Teepen, T., Yao, Z., Grifoni, M., and Dekker, C. **Carbon Nanotube Single-Electron Transistors at Room Temperature.** *Science*, vol. 293, 76-79 (2001).

[13] Fuhrer, M. S., Nygard, J., Shih, L., Forero, M., Yoon, Y. G., Mazzone, M. S. C., Choi, H. J., Ihm, J., Louie, S. G., Zettl, A., and McEuen, P. L. **Crossed Nanotube Junctions.** *Science* **288**, 494 (2000)

[14] Avouris, P. **Carbon Nanotube Electronics.** *Chemical Physics* 281, no. 2-3,: 429-45 (2002)

[15] Yao, Z., Dekker, C., and Avouris, Ph. **Electrical Transport Through Single-Wall Carbon Nanotubes.** M.S. Dresselhaus, G. Dresselhaus, Ph Avouris (Eds.): *Carbon Nanotubes*, Topics Appl. Physics. 80, 147-171 (2001)

[16] Martel, R., Derycke, V., Lavoie, C., Appenzeller, J., Chan, K. K., Tersoff, J., and Avouris, Ph. **Ambipolar Electrical Transport in Semiconducting Single-Wall Carbon Nanotubes.** Physical Review Letters, vol. 87, no. 25 (2001)

Chapter 3: Procedure

3.1 State of Project at Onset

When I began work on this project in January 2002 much of the apparatus had been set up, though no nanotubes had been successfully grown. The 1-inch Lindberg Blue tube furnace was operational with the capacity for both argon and methane flow. The AFM was also fully operational. Senior lab groups had attempted nanotube growth during the previous fall, without success. Their lack of success was almost certainly due to their choice of a catalyst material not suited to methane CVD growth, and the use of unoxidized silicon substrates. One result of the choice of catalyst and gas flows was a significant amount of carbon deposition on the quartz boat and tube, and very dirty samples.

3.2 Proceedings of My Work

3.2.1 Basic Setup/ Apparatus

Our tube-growth apparatus consists of a Lindberg/Blue TF55035A-1 high temperature tube furnace with UP150 electronic controller, 1' heating coil length, 1"x3' quartz tube and quartz boat. Initially installed in this setup were two gas bottles, methane and argon. Argon gas pressure is regulated by a Victor GPS270-80-580-BV regulator with right-handed male connector; methane pressure is regulated by a Victor GPS270-80-350-BV, which is the same regulator but with a right-handed female connector. Both gas flows are then controlled by Gilmont N092-04 flowmeters with stainless steel floats; these have air capacity of 460 to 4562 sccm. After passing through the tube, the gas flow is directed

into a fume hood through an oil bubbler flask (see Fig 2.) which allows visible detection of any gas flow.

Figure 1.
Our growth apparatus. From left to right: hydrogen, methane and argon bottles, Gilmont flowmeters for argon, methane and hydrogen, Lindberg Blue tube furnace.

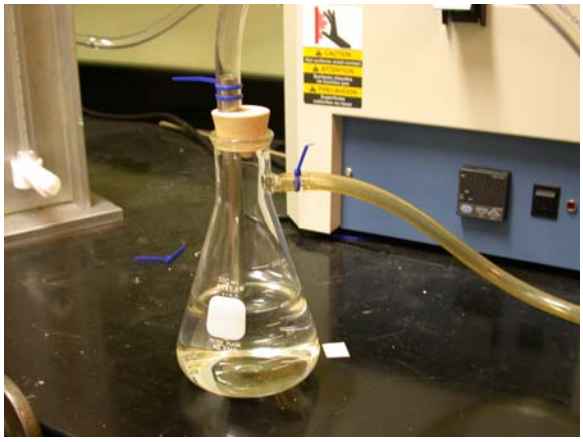

Figure 2.
Oil/Water bubbler

To enable silicon oxidation a second bubbler was placed in the flow-path before the tube entrance, and filled water rather than oil. Argon flowing through the bubbler picks up some water vapor and carries it into the furnace where to oxidize the substrate.

In order to add Hydrogen flow, a new flow-meter and regulator were purchased. We were able to fill an old Hydrogen cylinder, and so did not have to purchase a new one. The Hydrogen flowmeter is a Gilmont 02281 with stainless steel float and air capacity of 3 to 300 sccm. After mistakenly ordering a regulator with left handed female

thread—incompatible with our right handed male cylinder—a duplicate of our Methane regulator was ordered with the proper thread and connector.

A new Dell PC was purchased to run the LabVIEW software for controlling the data acquisition of fine electrical measurements. The LabVIEW software was installed, as was a D/A PCI card (National Instruments PCI-6052E multifunction I/O board). The setup was tested by alternately adjusting and measuring the output of the analogue output channel 0, and determined to be in working order.

We use a Digital Instruments AFM with Nanoscope IIIa controller, and Nanoscope software version 4.3 revision 8 for MS DOS.

3.2.2 Nanotube Growth

Methane Based Growth

In order to grow tubes with the setup available—which used methane as the carbon source gas—a suitable catalyst was chosen. The process used by Dai et al[1], involves a solution of $Fe(NO_3)_3 \cdot 9H_2O$, $MoO_2(acac)_2$, and alumina nanoparticles in methanol used as catalyst. This is also the method used by Paul McEuen's group at Cornell, with whom we have some contact and thus the potential for dialogue in case of problems. The alumina particles are a product called Aluminum Oxide C manufactured by the Degussa Company, and were available as a free sample.

While catalyst materials were being acquired, a sample of silicon was oxidized, using the water bubbler, for about 3 hours at 1000°C, which should produce oxide on the order of 3 microns thick[2]. The remaining silicon stains on the quartz boat and tube were also oxidized to SiO_2 by the first run, leaving both clean and clear. Though I did not

measure the oxide thickness, the color of the silicon surface had changed from silver to a deep blue, indicating the presence of oxide. Subsequent oxidations were done for .75 to 1 hours at 1000ºC.

Catalyst chemicals were mixed according to Dai et al.[1]: 0.02g $Fe(NO_3)_3 \cdot 9H_2O$, 0.005g $MoO_2(acac)_2$, and 0.015g of alumina particles in 15mL methanol. After stirring this solution for a full 24 hours and sonicating for one hour, a drop was applied to the previously oxidized silicon wafer. As per the Dai recipe, growth was done at 1000°C. The furnace was heated under Argon flow of about 1.5 sLm, and then the flow was replaced with 2083 sccm for ten minutes. Cooling was done in Argon. To monitor gas flows with a meter calibrated for air, the flow is adjusted by its density according to $Flow_{air} = Flow_{gas} \times GCF$, where GCF is the ratio of gas density to air density (This calculation was neglected for the first growth run). At first glance this sample appeared to have no nanotubes, and in many locations the surface is so rough that any nanotubes would likely be masked. But after some time under the AFM many tubes were discovered, mainly on what look to be clean silicon surfaces near the edges of large planes of catalyst particles (Figure 3).

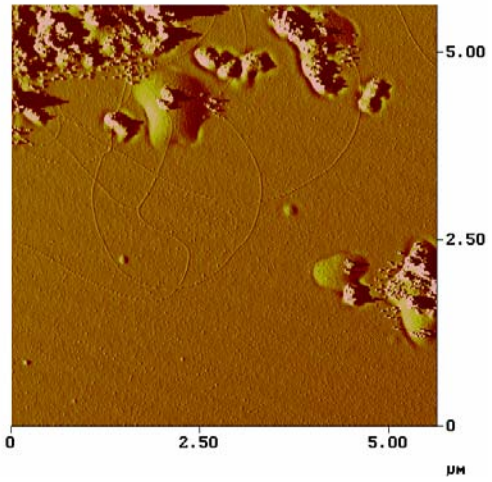

Figure 3.
Nanotubes growing near large catalyst particles.

These tubes were discovered after returning to Pomona from two weeks at Cornell. I also discovered that the gas flows used during growth on the first sample were different than expected because differences in gas density were neglected (the 2083 sccm reported above is in fact the correct flow, though I had expected 1500 sccm). Dai et al. report nanotube growth with between one and six sLm CH_4 during the growth phase; my next few growths were done in 3 sLm CH_4 during the growth phase, calculated using a gas correction factor (GCF) of 0.72 for CH_4.

The effect of this change was not clear because no nanotubes were growing on any samples at the time. None of the samples made since returning from Cornell had been oxidized, since no oxide was required for ethylene-based growth. However, an oxide layer does seem to be required for methane-based growth in our furnace; as soon as samples were prepared that had been oxidized for 1.5 hours at 1000ºC in 1.8 slm Ar/H_2O before catalyst deposition, nanotubes began to grow again. To discover the oxide requirement, the flow conditions of the original sample were duplicated, again unsuccessfully. The only difference between the samples with successful tube growth and those without was the presence of an oxide layer. A discussion of why oxide is required for growth can be found in the theory section. Eventually another growth was done in 3 sLm CH_4, and no nanotubes were found on the sample. Due to time constraints at the late date of the second test, the examination of this effect was far from exhaustive. More testing of the effect on flow rate should be a part of future work to maximize the density of tube growth.

Several steps were taken toward reducing the roughness of the catalyst deposited on sample surfaces to allow more surface area to be imaged with the AFM. The catalyst

solution was diluted by one half to reduce the concentration of large particles on the sample surface. This produced a visible change in catalyst density, but no significant change in the magnitude of roughness. The Al_2O_3 particles are large in comparison with the molecular $Fe(NO_3)_3 \cdot 9H_2O$ catalyst particles, and it does not seem to be possible to achieve the relatively smooth surface of the molecular catalyst samples (those using only $Fe(NO_3)_3 \cdot 9H_2O$) when using the preparation involving alumina particles.

In a paper subsequent to the one from which I culled our growth recipe, Dai et. al. add H_2 to their flow.[3] A small amount of H_2 co-flow slows the decomposition of CH_4, reducing the production of unwanted carbon compounds by pyrolysis. In case some of the sample roughness was due to unwanted carbon compounds, H_2 co-flow was added during growth. Because it is predominantly gas velocity that affects tube growth, the flows from Dai et al.[3] had to be adjusted so that the gas velocity in our 1-inch furnace would be the same as in their 4-inch furnace. Dividing their rates by 16 gives the desired flows to be 67.5 sccm CH_4 (GCF .72), and 8 sccm H_2 (GCF 3.61). H_2 was added at 10 sccm, and CH_4 flow was reduced to 300 sccm because our flowmeter is not accurate below that level. An additional annealing step was added before growth; 1 sLm Ar and 10 sccm H_2 are passed over the sample at growth temperature for 15 minutes. Samples grown under these conditions were noticeably cleaner, though no nanotubes could be found, and no nanotubes have grown on several samples where H_2 was flown during a pre-growth anneal or during actual growth. Due to time constraints further work here was also abandoned, but it should be possible to find levels of hydrogen that reduce the amount of amorphous carbon generated while still allowing growth.

Ethylene Based Growth

In June of 2002 I traveled to Cornell University to work with Paul McEuen's research group. I collaborated with Jed Whittaker, a student of Robert Davis at Brigham Young University. While at Cornell, Jed and I helped PhD candidate Scott Bunch refine a growth recipe for producing nanotubes easily picked up by the scanning probe microscope tip. This recipe follows that described by Lieber, et. al,[4] and uses only $Fe(NO_3)_3 \cdot 9H_2O$ as catalyst and C_2H_4 and H_2 during the growth phase.

To prepare the catalyst we mixed .006g $Fe(NO_3)_3 \cdot 9H_2O$ in 40 mL Isopropyl Alcohol. We also prepared two dilutions of this preparation, .006g $Fe(NO_3)_3 \cdot 9H_2O$ in 80 mL IPA, and .006g $Fe(NO_3)_3 \cdot 9H_2O$ in 160 mL IPA. Samples were prepared by dipping a clean silicon chip into the catalyst solution for one to three seconds, rinsing in pure hexane (Fischer H292-500) and then drying with N_2. Growth was done in a Lindberg Blue tube furnace with 2' heating coils and a 1"x3' tube. After heating to 700° in 1 sLm Ar, the sample was annealed for fifteen minutes in 100 sccm H_2 and 150 sccm Ar. 5.5 sccm C_2H_2 was then added for six minutes, followed by cooling in 1 sLm Ar. The furnace setup had electronic mass-flow controllers (made by MKS) to monitor the small gas flows accurately.

As can be seen in Fig. 4, samples produced with this growth method feature many nanotubes that grow away from the substrate, unlike the methane-based process where tubes generally lie flat. In order to "pick up" a nanotube from one of these samples, we simply scanned across an area between fifteen and twenty microns on a side. Nanotubes are strongly attracted to silicon; they stick to sample surfaces and they also stick quite well to the silicon surface of the scanning probe microscope tip. Because the tubes grow

off of the surface, when the probe tip passes through a group it occasionally snags a tube. Any “pick up” can be easily seen during scanning because the tube dragging across the surface produces a large amount of noise.

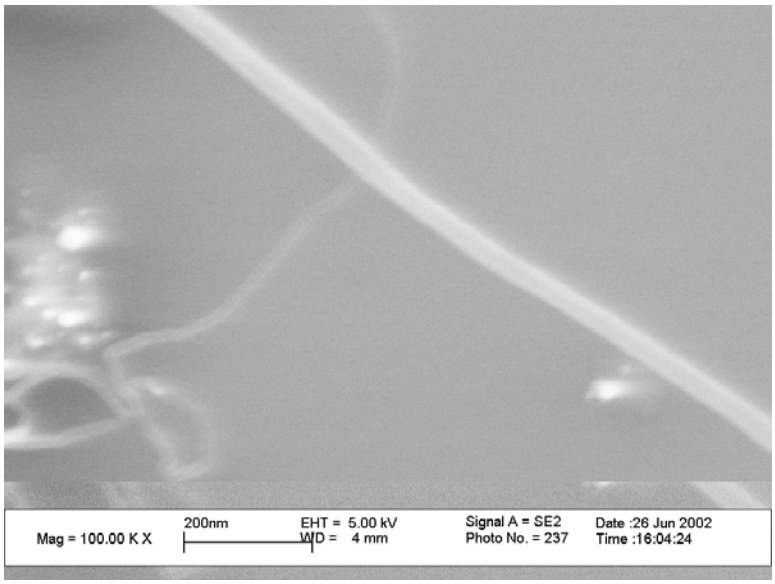

Figure 4.
SEM image taken by David Tanenbaum and Robert Davis. Image shows how nanotubes curl away from the substrate.

This noise renders the scan indecipherable, and the tube must be shortened to a length that offers more rigidity before it will function well as a sensing tip. The procedure for shortening attached tubes is simple: shake the tip vigorously. Increasing the scan size to about 20 microns and scanning at 30 Hz for a few seconds either shakes the nanotube off of the tip, or it breaks the tube down to a smaller size as it mows through the junk and other tubes on the surface. When the shaking successfully modifies the tube, the image is again clear when the scan is returned to a normal rate. Often several high-frequency shakes are required before the tube will function properly.

During my two-week stay various aspects of the sample prep and growth processes were adjusted to maximize the yield of tubes while keeping the amount of carbon junk that interferes with scanning to a minimum. Small changes in sample

preparation had noticeable affects on the quality of the final surface. If the Hexane used to rinse excess catalyst from the surface was not of very high purity it left behind residue as it evaporated that was visible during scanning. The best of our samples had surfaces that were smooth, and contained on the order of ten nanotubes in any 100 square microns.

3.2.3 Patterned Catalyst

In order to make any electrical measurements on nanotubes metal electrodes must be brought into contact with both ends of a tube. In the best method for making such contacts that is affordable for us metal is evaporated over both ends of a nanotube that has already grown on a surface by CVD. To be successful, this method requires confidence that nanotubes can be grown in essentially the same configuration in consecutive samples. If such consistency is not possible, a new metal film configuration would be required for each sample, along with a great deal of additional hunting and pecking for nanotubes in order to properly align the metal films. With a CVD growth process it is relatively straightforward to localize tube growth if one can pattern the catalyst on the sample surface.

One suggested method for producing catalyst patterns was microcontact printing. While at Cornell I tried printing catalyst on several samples using PMMA stamps; one with ten-micron lines and ten-micron spaces, another with one-micron lines and one-micron spaces. Dipping the stamps in catalyst and then stamping them on the surface like a normal rubber stamp did not work well—it was too hard to get a clean edge. By cutting the stamp perpendicularly to the pattern with a razorblade, the channels could be exposed

directly to the edge. If the stamp were then clamped to the silicon surface with a locking tweezer, a small drop of catalyst placed next to the stamp flowed by capillary action into the channels. When the solvent evaporated, ridges of catalyst with clean edges remained.

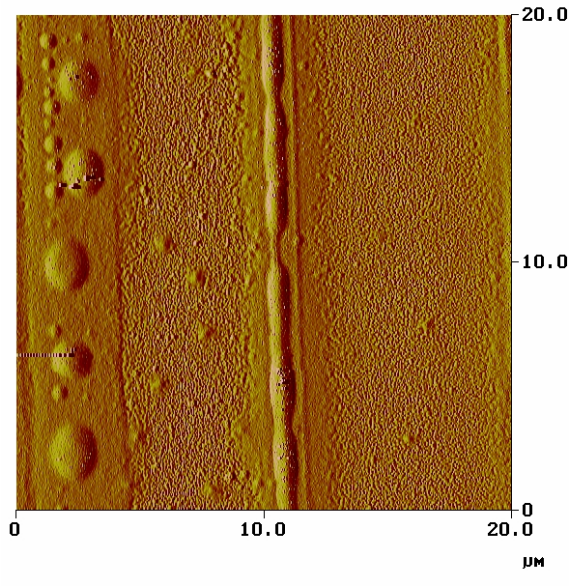

Figure 5.
AFM image of catalyst patterned with a microcontact stamp. The stamp features are alternating lines and spaces, each ten microns wide. No nanotube growth is evident in this region.

Several such samples were prepared and run through the furnace with mixed results; an example can be seen in Fig 5. The usefulness of patterned catalyst is obviously contingent upon consistent and predictable tube growth. With such growth one can then make a process that will deposit metal film in areas where there is a high probability it will overlap a nanotube in many similar but not identical samples. While in almost all cases many tubes grew on the samples patterned with stamps, they did not grow on the patterned area. Neither did they grow from the edge of the catalyst ridge onto the adjoining clean surface, which would have been ideal. Instead all growth was in the excess catalyst outside of the stamped area. Because there are no edges in these regions there is no way to determine reliably where a tube will grow, making it much

harder to successfully cover both ends of a tube with metal. For these reasons this method of patterning catalyst was pursued no further.

A more robust method for patterning catalyst involves using lithography to pattern catalyst into small islands. Paul McEuen's group has developed a very reliable process (based on work by Dai et al.[1]) involving e-beam lithography on PMMA to pattern their catalyst into micron-sized rectangular "pads," and some groups now use anodized silicon to make large clusters of tubes.[5] Prior to winter 2002 the only method we could afford for patterning catalyst was microcontact printing. As mentioned above my attempts at this did not lead me to believe it would be successful.

In January of 2003 David Musgraves (PO '03) was making significant progress in the development of an optical lithography process that uses a PC to control a digital projector focused through a trinocular-head microscope to pattern standard Novolak-based positive photoresist. We can spin-coat photoresist and other polymers onto silicon using a Krupps variable-speed blender modified with an aquarium vacuum pump, an apparatus developed a few years earlier by David Tanenbaum. The microscope setup could then pattern features as small as 50 microns—certainly small enough already to be useful, and the feature size was shrinking as Dave refined his procedure. This apparatus could perform the lithographic steps necessary to create catalyst pads like those used effectively in the McEuen lab and elsewhere.

PMMA was the first choice for resist because it is clear from previous work that it does not interfere with the catalyst or with tube growth. Unfortunately PMMA is not especially responsive to visible light. After exposing several films to blue light—which

is brighter than violet in our setup, though the photons have lower energy—for 30 min, it was clear that we could not pattern PMMA under reasonable conditions.

The Novolak based resist used by Dave was attractive because much of the work in determining exposure times had already been done, and work was still in progress to improve features. There are several problems with this chemical however. Primarily and most threatening, there is no widely available literature, if there is any at all, in which someone has used this chemistry in conjunction with a nanotube growth process; PMMA is clearly the resist of choice. It is therefore unclear whether residue from optical photoresist would interfere with nanotube growth chemistry.

Another problem: though it is baked for thirty seconds at 90ºC directly after spin-coating, the resist remains somewhat soluble in the methanol solvent supporting the catalyst mixture. Before work could begin on patterning resist and making catalyst pads this solubility issue would need resolution. By baking the resist for 25 seconds at 170ºC the resist is rendered impervious to methanol and many other solvents, including the acetone used by Dave to strip the resist after exposure and development. Even after warming the acetone near its boiling point the resist was unmoved. Fortunately there are many commercial chemicals designed for this sort of application. Cyantek, a subsidiary of Rockwood, manufactures an NMP-based photoresist stripper called RS-100 which they offered as a free sample. The stripping process proposed by Cyantek engineers and distributed with the sample involves heating some of the stripper to 90ºC. After time in the hot bath the sample is transferred to a cool stripper bath before it is rinsed with water. This process removes photoresist baked at 170ºC for 1 minute after about two minutes in the hot bath.

Now that any photoresist could be removed, focus could be shifted to the patterning process. "Mask" screens were created in Microsoft PowerPoint. According to work by Dave Musgraves[6] the best "color" for exposing our resist (which is made up of 1 part Novolak resin to 4 parts DQ and 10 parts Cellosolve acetate (solvent)) is RGB (0,0,255). Mimicking the layout of Paul McEuen's group, I designed slides with six small catalyst pads, each on the order of 400 μm^2. These can be seen in Fig. 6.

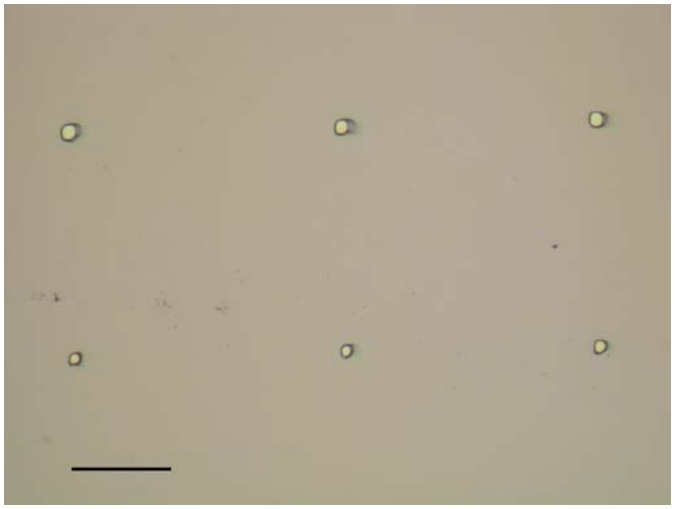

Figure 6.
An image of the catalyst pad pattern, scale bar is approximately 500 μm.

In PowerPoint these were created with lines of width 2.75pt, or 4 pixels, and length 0.04", which projects as 4 pixels; each pad has a 12 pixel area. The actual projected size of the pattern on the substrate is approximately 27 microns per side, or 900 μm^2. This pattern exposes in 120s, and is developed in 0.2M NaOH for 60s. It is also possible to pattern smaller pads; several samples have been made with lines of width 2.0pt, and height 0.005", corresponding to about nine square pixels. These require 180s to expose and develop in 60s. It may be possible to pattern even smaller catalyst islands in the resist, though the pads might not survive the subsequent resist stripping process.

After patterning and developing samples, they are baked at 170ºC. The first samples were baked for about 45s. Resist baked for this long is hard enough that the methanol catalyst mixture simply dries on the surface without visibly damaging the resist. To strip resist that has been baked this long requires up to 150s in hot RS-100 (hot-plate temp=110ºC, liquid temp about 90ºC). If the sample is placed in a cold RS-100 bath for a few seconds after the hot bath, rinsed with water, and then dried with a compressed dry gas "dust-gun," the sample surface dries cleanly. Under magnification with an optical microscope the catalyst pads are clearly visible at 5x, with area generally between 100 and 500 μm^2. At 20x individual catalyst grains can be seen clearly.

After several of these samples have run through the furnace for nanotube growth using the standard method, no tubes have been found, though control samples in the same growth run do have nanotubes. Nanotube growth chemistry is complicated enough that it is very likely the resist stripper is interfering in some way, either actively during growth, or by altering the catalyst chemistry.

To minimize the effect of the latter, the time of the 170º bake was reduced to between 10 and 15s. With this shorter bake time the photoresist is damaged visibly by the methanol in the catalyst preparation, leaving a cloudy-looking surface and new interference fringe patterns that suggest a change in resist thickness. Happily the patterned edges appear unharmed under magnification in the optical microscope, so the samples should retain full utility. Resist baked for 15s can be stripped in hot RS-100 in just less than one minute. If the sample is baked at 170º for only 10s, the resist will strip in hot acetone (plate temp 90º) in 10-15s. Acetone is a volatile, combustible, and toxic

chemical. Clearly heating it to its boiling point is unsafe; any heating should be limited and very closely monitored, as was the case here.

Despite the shorter strip times, of four samples placed in the furnace none showed hints of tube growth. In order to learn a little more about what part of the process is inhibiting growth, a drop of catalyst was deposited on three clean (and oxidized) silicon samples. One of these was then dipped in hot RS-100 for 60s, another in hot acetone for 15s, and the final was placed in the furnace as a control. Nanotube growth was observed in both the control and the acetone-dipped sample, though not the sample dipped in RS-100. This seems to confirm that RS-100 interferes with growth chemistry, though it is encouraging that acetone (and probably similar solvents) does not. The tube density on these samples was low, explaining why no tubes were found previously on the acetone-stripped samples: the total catalyst surface area comprised of the small islands was not enough for a noticeable number of tubes to grow. With further work it is probable that the growth density could be increased, and tubes could be observed to grow from the patterned islands.

---

[1] Kong, J., Soh, H. T., Cassell, A. M., Quate, C. F., and Dai, H. **Synthesis of individual single-walled carbon nanotubes on patterned silicon wafers.** *Nature* **395**, 878 - 881 (1998)
[2] Campbell, Stephen A. *The Science and Engineering of Microelectronic Fabrication.* Oxford University Press: Oxford. 1996
[3] Franklin, N. R., Li, Y., Chen, R. J., Javey, A., and Dai, H. **Patterned growth of single-walled carbon nanotubes on full 4-inch wafers.** *Applied Physics Letters* Vol. 79, p. 4572 (2001)
[4] Hafner, J. H., Cheung, C.-L., Oosterkamp, T. H., and Lieber, C. M. **High-Yield Assembly of Individual Single-Walled Carbon Nanotube Tips for Scanning Probe Microscopies**. *The Journal of Physical Chemistry B* 105, 4, 743 (2001)
[5] Wind, S.J., Martel, R., and Avouris, Ph. **Localized and Directed Lateral Growth of Carbon Nanotube From a Porous Template.** *Journal of Vacuum Science & Technology B* 20, no. 6, 2745-8 (2002)
[6] Musgraves, J. D., and Tanenbaum, D. Senior thesis, to be "published" in *Pomona Physics Library*, vol. 2003

Chapter 4: Results

4.1 Methane Based Nanotube Growth

The growth method that produces the highest concentration of SWNTs to date involves using catalyst solution prepared with 0.02g $Fe(NO_3)_3 \cdot 9H_2O$, 0.005g $MoO_2(acac)_2$, and 0.015g of alumina particles in 15mL methanol. This is stirred for 30 min and sonicated for 30 min before a drop is placed on a clean oxidized sample of silicon. No tests have been performed to determine how growth depends on oxide thickness, but growth has been observed on commercially prepared samples with a .2 μm oxide layer, and homemade samples with a layer that should be on the order of microns thick. After depositing catalyst material on the substrate, samples are heated to 1000°C in 1 sLm Ar. Growth takes place in 2.08 sLm CH_4 for ten minutes.

The samples produced by dropping catalyst directly onto the surface have large areas of roughness where catalyst particles have conglomerated. The magnitude of this roughness is on the order of 20 nm or greater, making any AFM image of this surface very difficult to interpret. These rough areas frequently have sharp edges, and a scan of the smooth surface near such an edge reveals roughness on the order of 10 nm, and frequently the growth of SWNTs. The average density of tubes in this region is about 3 per 225 μm^2. Figure 1 shows such a region. In general these tubes are high quality SWNTs, of length ranging from 5 to 25 μm. That they are in fact SWNTs can be verified from measurements of their diameter.

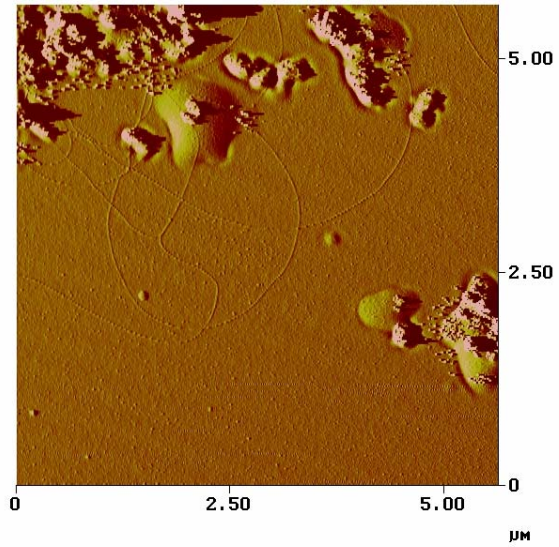

Figure 1.
SWNTs grown in methane using catalyst prepared with $Fe(NO_3)_3 \cdot 9H_2O$,$MoO_2(acac)_2$, and alumina particles.

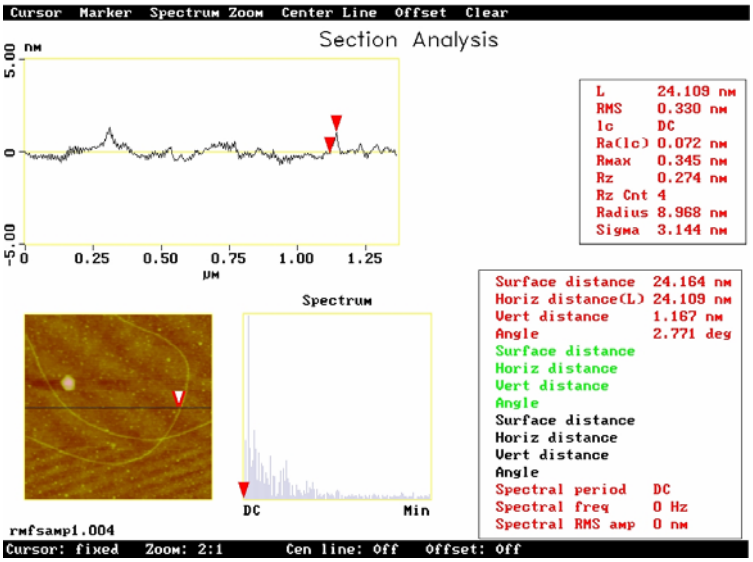

Figure 2.
Section analysis of crossed tubes visible at bottom of Fig.1. Tube diameter is 1.167 nm.

Careful measurements of tube diameter can be made using height data collected with the AFM. Cross sections of this data can be taken perpendicular to a target nanotube, as in Fig. 2. Horizontal travel across the tube is generally much larger than vertical travel, due to the low aspect ratio of the scanning probe tip. When the probe reaches a sharp edge such as a nanotube—whose diameter is significantly smaller than the probe's—the horizontal travel distance includes the radius of the probe tip. Since a

nanotube has two such edges the probe radius is measured twice, significantly distorting the horizontal length of the tube. The vertical travel measured by the tip is not subject to such distortion however, and so provides an accurate measure of the tube's diameter.

4.2 Patterned Growth (Methane Based)

SWNT growth can be consistently produced on bulk samples, but despite success at producing catalyst islands of reasonable size and density no growth has been observed from patterned catalyst. Catalyst islands as small as 225 μm^2 were successfully patterned in the photoresist, but because the catalyst does not fill resist patterns fully and the resist stripper is not very sensitive, features this small did not carry through to the end of the process well. For these reasons most samples were patterned with 400 μm^2 features. After depositing catalyst and stripping, the area of most remaining pads was generally on the order of 300 μm^2. Figure 5 and 6 show catalyst pads ready to go into the furnace for growth.

After attempting growth on several samples whose resist was stripped with RS-100, no nanotubes could be found. Reductions in the length of the RS-100 strip showed no improvements. Reducing the 170º bake to 10 s enabled the resist to be stripped with hot acetone, though no tubes were observed on several samples of catalyst pads that had been stripped in acetone. In a control experiment, one drop of catalyst was placed on three oxidized silicon samples and allowed to dry. The first sample was bathed in RS-100 for one minute, the second in hot acetone for 15s, and the third was left as a control. After all three samples underwent standard CVD growth no nanotubes were discovered

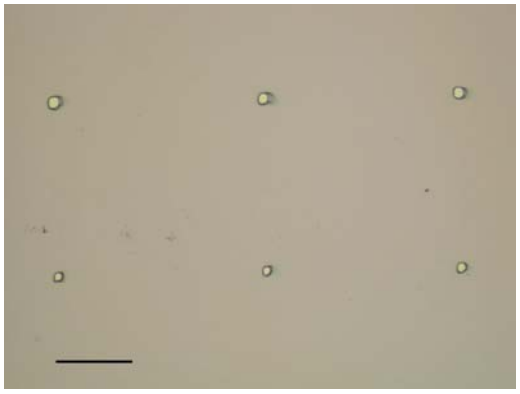

Figure 3.
Patterned photoresist before catalyst is deposited. Scale bar is approximately 500 µm

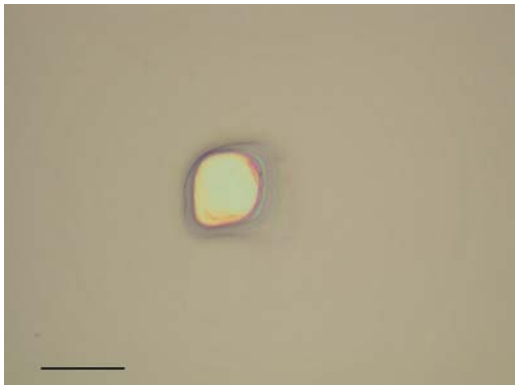

Figure 4.
Close up of catalyst pattern showing the typically clean exposed edges. Scale bar is approximately 20 µm

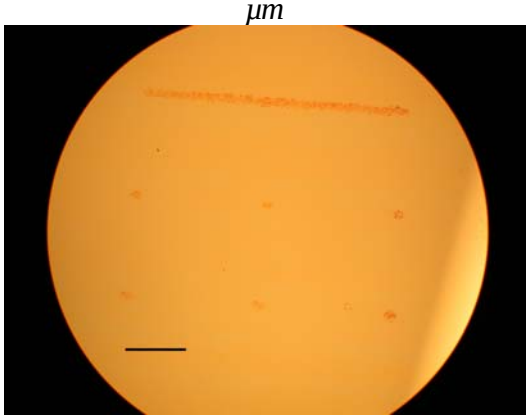

Figure 5.
Image of catalyst pattern after resist has been removed with RS-100. Scale bar approximately 330 µm.

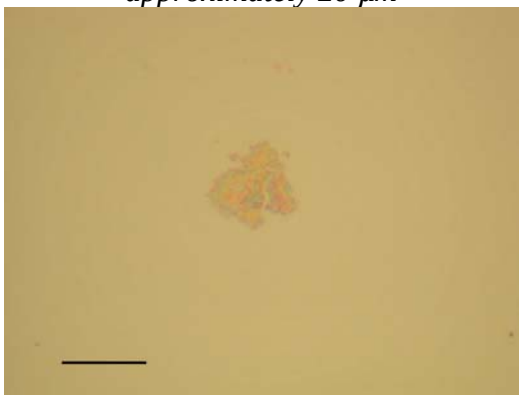

Figure 6.
Close up of Catalyst pad from Fig. 5. Scale bar is approximately 20 µm.

on the RS-100-dipped sample, indicating that RS-100 strongly inhibits tube growth. Small numbers of nanotubes were discovered on the acetone-dipped sample, and moderate growth was observed on the control sample. From this experiment can be concluded that nanotube growth is unlikely on samples immersed in RS-100. Nanotubes will grow on samples immersed in hot acetone for 15s, but the growth density is reduced. For samples with small catalyst area, like those whose catalyst has been patterned, the

probability that a tube will grow from one of the pads is low under current growth conditions.

The results of a final growth done to begin determining steps by which tube density might be increased were inconclusive. In this experiment three samples were prepared with a drop of catalyst deposited on all three. One was then dipped in hot acetone for 5 s, another for 10 s, and a third was left as a control. During CVD growth the amount of methane flow was increased to 3 slm, and no tube growth was exhibited by any of the three samples.

The principle problem with our current methane-based growth is low tube density. This density must be increased before growth can occur regularly on the small catalyst surface area of patterned samples. Simple (though time consuming) experiments with CH_4 and H_2 flow rates, growth time, and perhaps growth temperature should lead to growth parameters that increase the number of tubes per unit area of catalyst surface, until growth is dense enough that one would expect to observe growth from small catalyst islands.

4.3 Ethylene Based Nanotube Growth, Nanotube Tips

The best method for growing samples in Ethylene uses catalyst solution prepared by mixing 0.006g $Fe(NO_3)_3 \cdot 9H_2O$ in 40 mL Isopropyl Alcohol. A clean, unoxidized sample is dipped in the catalyst and then rinsed with high purity (Fischer H292-500) hexane, before it is dried with a nitrogen blast. Samples are heated to 700°C in 1 sLm Ar, and then annealed for 15 min in 150 sccm Ar and 100 sccm H_2. For growth 5.5 sccm C_2H_4 is

added to the anneal mix for 6 min. This produces a relatively smooth surface with large numbers of nanotubes growing away from the surface, as can be seen in figure 7.

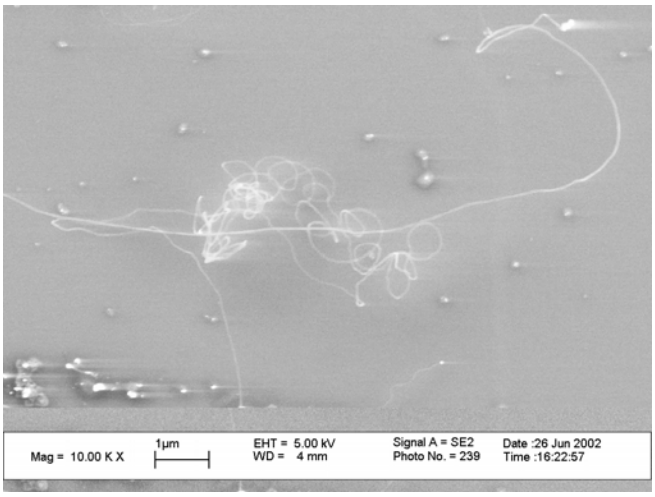

Figure 7.
An SEM image taken by Prof. David Tanenbaum and Robert Davis. The sample was prepared by Jed Whittaker according to the methods described in the procedure section of this document. The tubes on this sample can be seen to grow away from the silicon surface.

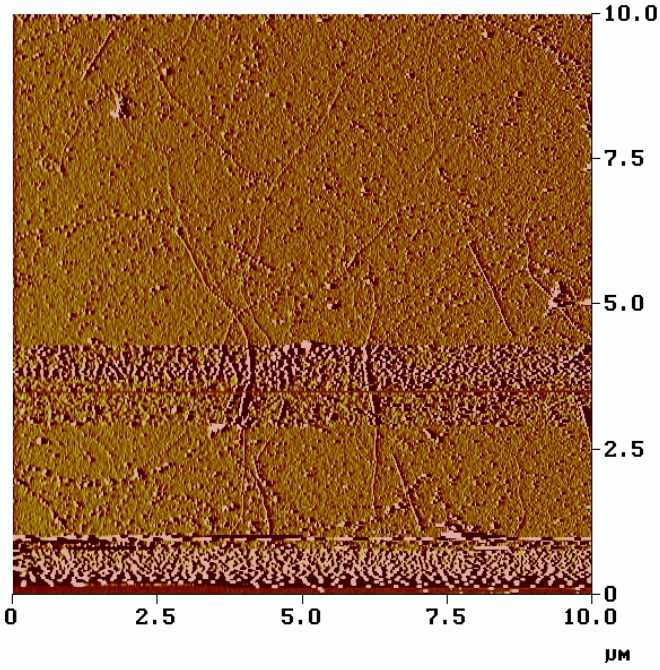

Figure 8.
Image of nanotubes grown in ethylene. Tube density is high, though amorphous carbon and nanotubes protruding from the surface often add noise to scans.

The surface does not feature the large alumina particles found in the other catalyst preparation, but even after refining growth parameters to clean the samples significantly

there remains carbonaceous junk that tends stick to the AFM probe. Noise due to such interaction plagues many scans of the surface, as can be seen in Fig. 8.

The interesting feature of growth by this method is the ability to pick up a nanotube with the AFM probe, and subsequently image with the nanotube acting as tip (the process of picking up tips is described in greater detail in the procedure section). Images taken with nanotubes look very similar to those acquired using conventional silicon tips. Figures 9 and 10 show the cross sections of two scans of similar nanotube samples taken with probe tips of vastly different radius. Figure 9 was probably captured with a traditional silicon tip, while figure 10 was captured with a nanotube tip. The distance measured between the two red markers is given by Horiz. Distance(L) in the figure.

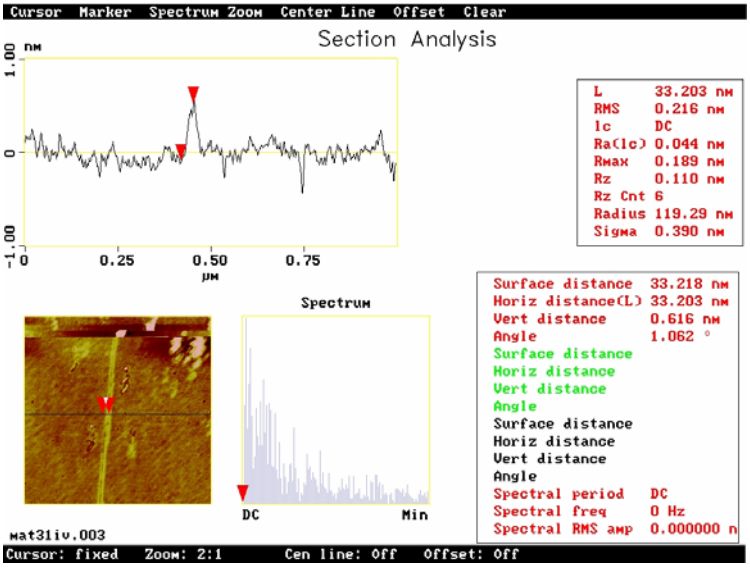

Figure 9.
An image of a nanotube taken with a traditional silicon probe tip. Note the horizontal distance of 33 nm

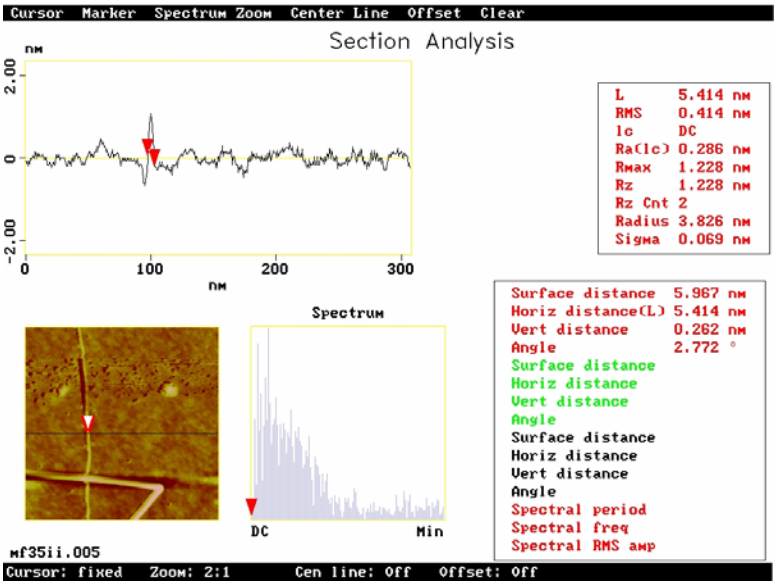

Figure 10. *An image of a nanotube scanned with a nanotube tip. Note the horizontal distance between markers is 5.414 nm.*

In figure 9, this distance measures the radius of the sample tube, and reads 33 nm. In figure m the markers correspond to the diameter of the sample tube, which is measured to be 5.14 nm. The two samples were grown in the same manner and feature roughly the same tube characteristics; it is therefore unlikely that the tubes vary so wildly in size. Instead, much of the difference is due to the diameter of the scanning probe. This is corroborated by the vertical distance measured between the markers of Fig. 9, which gives the diameter of the tube on the surface to be approximately 0.3 nm, which is probably somewhat smaller than the actual tube diameter due to some compression of the sensing nanotube. The significantly increased horizontal resolution of Fig. 10 is the result of scanning with a nanotube attached to the AFM tip. 5.414 nm is the lowest measurement of horizontal distance across a nanotube that we observed, with other low measurements of 8 and 10 nm.

If the diameter of the tube lying on the surface is approximately 0.6 nm, then we can make an estimate of the diameter of the scanning probe. A typical measurement of

tip radius is given by the full width at half maximum height.[1] The cross section of Fig. 10 is slightly wider than the full width at half max, so the tip radius is roughly 5 nm. Because of their extraordinarily high aspect ratio, nanotube tips are exceptional at resolving small objects and objects with sharp edges.

---

[1] Hafner, J. H., Cheung, Ch-L., Oosterkamp, T. H., and Lieber, C. M. **High-Yield Assembly of Individual Single-Walled Carbon Nanotube Tips for Scanning Probe Microscopies.** *J. Phys. Chem. B,* Vol. 105, No. 4. 745 (2001)

Chapter 5: Conclusions

This was an ambitious project for a senior thesis. As described in the introduction, the creation and characterization of a nanotube Coulomb blockade device requires work in several different areas, including nanotube growth, lithography, sophisticated AFM microscopy, and sensitive electrical measurement. The procedures for each of these steps are non-trivial, and only preliminary work had begun on nanotube growth before I began my work.

Though it is still far from completion, significant work on the project has been accomplished. The CVD growth of single-walled carbon nanotubes was consistently realized using methane as source gas and a solution of 0.02g $Fe(NO_3)_3 \cdot 9H_2O$, 0.005g $MoO_2(acac)_2$, and 0.015g of alumina particles in 15mL methanol as catalyst. The tubes produced by this growth are high quality SWNTs with diameters between .5 and 3 nm, suitable for measurements of quantized conductance and the dependence of conductance on the tube-wall structure.

In addition, catalyst was lithographically patterned into small squares whose area is approximately 400 μm^2, suitable for controlled nanotube growth that allows electrodes to be easily deposited over grown nanotubes. It seems that the average density of current nanotube growth is low enough that nanotubes do not grow on the patterned islands. Provided that Acetone is used to remove photoresist prior to growth however, test results show that it is possible for a patterned sample to grow nanotubes, though none have to date. Adjustments in gas flow during the growth phase should increase the average growth density to a point where tubes can be found on the patterned samples. A more detailed discussion of findings can be found in the results section.

In summary, enough progress has been accomplished that it should only take two or three more thesis students to measure quantized conductance in a nanotube! It is remarkable just how much time it can take to make progress in a multi-stage experimental process like the one detailed in this report. In a project with many disparate components there is a surprising amount of troubleshooting work required simply to retain the present level of functionality, whatever that may be. When one does not work in lab every day, as will be inevitable in a liberal arts setting like Pomona College, it seems that progress is wrested from nature only haltingly. Hopefully the findings presented here will give some momentum to the next student to take up this cup; certainly they will provide a solid base from which to begin.

5.1 Acknowledgements

I wish to thank the Pomona College Physics Department for eagerly providing knowledge and assistance at all hours. Special thanks to my advisor Dr. David Tanenbaum for valuable advice, and for generously sharing his family's time with me in Ithaca. Thanks also to Dr. Alfred Kwok for assistance with job-hunting and camping gear, to Dave Musgraves for help with lithography and staying awake (and occasionally wasting time), and to Erin Grant for being a good sport and spending time with me in the basement. Finally, thanks to my fellow-travelers, the PO Physics class of '03 for support and friendship.